Journal of Sound and Vibration 329 (2010) 5489–5500

Contents lists available at ScienceDirect

Journal of Sound and Vibration

journal homepage: www.elsevier.com/locate/jsvi

Statistics of resonances and time reversal reconstruction in aluminum acoustic chaotic cavities

Oleg Antoniuk *, Rudolf Sprik

van der Waals-Zeeman Instituut, Universiteit van Amsterdam, Valckenierstraat 65, 1018 XE Amsterdam, The Netherlands

ARTICLE INFO

Article history:
Received 15 June 2009
Received in revised form
11 June 2010
Accepted 12 July 2010
Handling Editor: Y. Auregan
Available online 13 August 2010

ABSTRACT

The statistical properties of wave propagation in classical chaotic systems are of fundamental interest in physics and are the basis for diagnostic tools in materials science. The statistical properties depend in particular also on the presence of time reversal invariance in the system, which can be verified independently by time reversal reconstruction experiments. As a model system to test the combination of statistical properties with the ability to perform time reversal reconstruction we investigated chaotic systems with time reversal invariance using ultrasonic waves in aluminum cavities. After excitation of the samples with a short acoustic pulse the reverberation responses were recorded and analyzed. In the analysis of the spectral density of the recorded responses we explicitly included the fact that not all resonances are detected. Reversibility of the excited wave dynamics in the cavity after a time delay was studied by reconstruction of the excitation pulse in time reversal experiments. The statistical properties of resonance frequencies in the cavities were obtained from the reverberant responses. The distribution of the transmission intensities displays random division of intensity between cavity waves in narrow frequency bands. The distribution of frequency spacing between neighboring cavity resonances and the spectral rigidity agree with the predictions for the Gaussian Orthogonal Ensemble. This agreement is achieved if a fraction of typically 25 percent of resonances is not detected in the experiment. The normalized amplitude of the pulse that is reconstructed in the time reversal experiments decays exponentially with the time delay between the original excitation pulse and the end of the reversed oscillation track. The exponential behavior exists for time delays longer than the inverse of the nearest neighbor resonance spacing.

1. Introduction

Acoustic wave propagation is present in nearly all materials and structures. Particularly the statistical properties of scattered acoustic intensity can be used for non-destructive testing of materials and mechanical structures. Applications are e.g. monitoring quality and aging of building materials, tuning cars and testing computer hard drives [1].

The statistical approach [2,3] to describe properties of eigenvalues (i.e. resonant frequencies and energy levels) and eigenfunctions of complex Hamiltonian systems can be applied to interpret the properties of acoustic waves in complex systems. In general the associated wavefunctions of the resonant modes belong to several independent subspaces. E.g. each

* Corresponding author. Tel.: +31 642474541; fax: +31 205255788.
E-mail address: o.a.antoniuk@uva.nl (O. Antoniuk).

0022-460X/$ - see front matter © 2010 Elsevier Ltd. All rights reserved.
doi:10.1016/j.jsv.2010.07.010

subspace may consist of wavefunctions localized in separate parts of real space or wave functions with common symmetry as in case of sequence of wavefunctions in a rectangular cavity described by two independent wavenumbers [2].

The combined resonance frequencies of all the modes are than most likely uniformly distributed with a Poisson distribution for the resonance frequency spacing. I.e. the statistical properties of the resonance frequencies in a small enough frequency band with constant density of resonance frequencies should be the same as for randomly chosen values uniformly distributed within this frequency band. However, resonance frequencies of a classically chaotic system that has only exponentially diverging trajectories covering all the phase space (what leads to a sequence of modes described by a single wavenumber), should show level repelling [2] leading to a reduced probability of finding small frequency spacings.

The statistical properties of resonance frequencies in chaotic systems can be described by Random Matrix Theory (RMT) [2]. The RMT is applicable to scattering of various kinds of waves, in particular also for acoustic waves [4]. For acoustical waves the Hamiltonian corresponds to the operator of the acoustic wave equation describing the displacement and velocity of the elastic motion. In RMT statistical properties of the levels are obtained for different models of random Hamiltonian matrices with appropriate symmetries. Examples of such symmetries are the time reversal invariance of the underlying wave equation and geometrical symmetries in the cavity. For example a thin 2D plate of irregular shape when it has one or two symmetry planes normal to its surface, studied in [5,6].

To accurately measure the spacing distribution between nearest neighbor resonances, all resonances in the system should be carefully identified. In practice the finite resolution of the experiment causes that a fraction of resonances are "lost" in determining the statistics. Also damping and mismatch in coupling between the cavity and the transducers hampers the identification of all modes. The ability to identify the distributions when accounting for lost levels expands the applicability of the statistical analysis in realistic situations. The effect of lost modes on the level statistics has been studied for the quantum mechanical problem in [7] but not for acoustics in 3D metal cavities. Accounting for lost levels involved complicated fitting procedure using a few approximations. Here we consider effect of lost levels by comparing the experimental data to statistical simulation.

There have been reported acoustic experiments [2] when the issue of the lost levels plays an important role, however, only a few quantitative descriptions of the lost levels have been published yet (e.g. article [8] by Enders et al. about states in heavy deformed nuclei and article [9] by Nogueira et al. about acoustic plate resonators).

For a system with time reversal invariance the evolution of a propagating pulse can be traced back by reversing all outgoing waves in time [10]. The reconstructed pulse is a combination of the refocused signal and the ongoing evolution of the waves after the reconstruction. In a cavity this mechanism of reversing all outgoing waves applies to even a single transmitter and detector pair [11].

The current paper reports on the statistical properties of intensity transmission coefficients, resonance line widths and resonant frequency spacings for non-integrable elastic waves in aluminum cavities with time reversal invariance. The experiments are conducted in the ultrasonic range (200. .450 kHz) by pulse excitation in the aluminum cavities (Section 2). A short introduction to RMT is given in Section 3 including the effects of "lost levels" on the statistics. We compare statistics obtained from the experimental results with the RMT prediction for random Hamiltonian with time reversal invariance in Section 4. Finally we also show how efficiently the original excitation pulse is recreated in the experiment by replaying a reversed part of the recorded response after a delay with respect to the excitation pulse. Time-reversal experiment gives a clear measure of time reversal invariance in the system on different time scales.

2. Experiments with aluminum cavities

2.1. Material properties and design of samples

A set of identical aluminum cubes with a side length of 20 mm where used to construct different chaotic cavities. An asymmetrically placed well was drilled in cavities Nr. 1 and Nr. 2 to remove the cubic symmetry. An extra side corner was removed from cavity Nr. 2 (see Figs. 1 and 2) to lower the symmetry even further. Cavity Nr. 1 has one symmetry plane. Cavity Nr. 2 does not have any symmetry properties like rotation axes, reflection planes and will only have chaotic sets of geometric ray trajectories and a non-separable wave equation.

The longitudinal wave velocity was determined for the used aluminum by measuring first arrival of the acoustic pulse through the stack of plates (cubes) of different width. There is also an agreement between five lowest resonances of the symmetric (unperturbed) cubic resonator of the same aluminum and precise calculations [12], what gives values of the longitudinal and transverse sound velocities approximately of 6400 and 3200 m/s.

2.2. Sample support and transducer holders

To reduce damping in the system a very light low mass support is used. A slab of low mass density packing material supports three small polystyrene pieces which touch the cavity only in three points from the bottom. Small changes in the position of the support did not influence the transmission spectrum and the measurements are as close as possible to the an aluminum cavity with free boundary conditions.

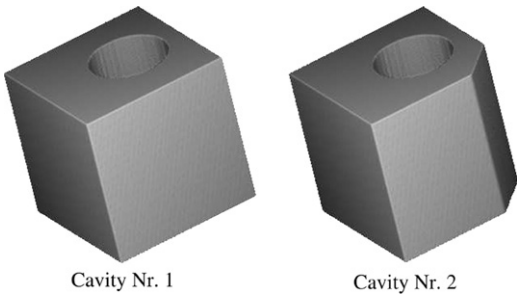

Fig. 1. The cavities used in the experiment are made out of aluminum cubes with a cube side size of $d=20$ mm. The symmetry of the cubes is broken by additional features such as an asymmetrically placed cylindrical well (both cavities Nr. 1 and Nr. 2) and a removed side corner (cavity Nr. 2). The radius of the well is 5 mm and its depth is 18 mm. The center of the well divides two orthogonal sides of the square face of the cube as 0.5:0.5 and approximately 0.6206:0.3794. The removed side corner reduces each of two adjacent sides of the square face of the cube by 5 mm.

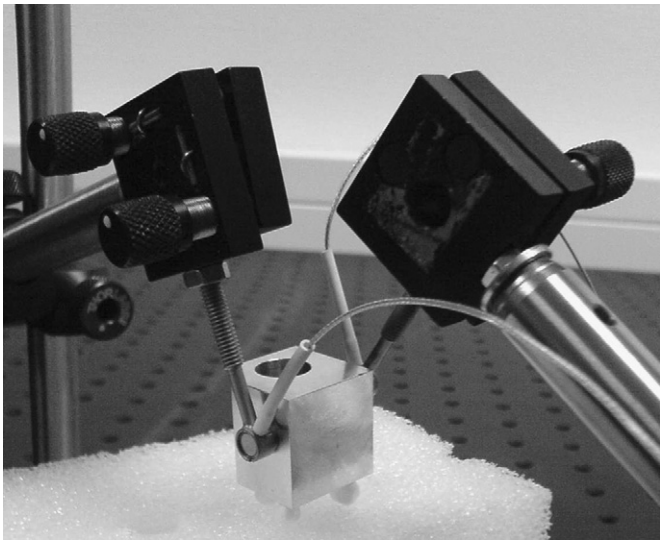

Fig. 2. Picture of the sample, transducers connected to it and transducer holders.

To satisfy the best possible alignment of piezoelectric transducers, the optical mirror holders with regulating screws are used as shown in the Fig. 2. Slight tuning of the alignment of the transducer holder with the regulating screws enables to reach the highest possible output signal.

2.3. Measurement instruments and procedures

The schematic of the experimental setup is shown in Fig. 3. An Agilent 33220A 20 MHz Function/Arbitrary Waveform Generator (AWG) generates signals driving the piezoelectric source transducer connected to the cavity using oil as couplant. It generates a voltage pulse of one period of 400 kHz sine shape to excite the sample. A Thurlby Thandar Instruments WA 301 Wideband Amplifier is used as the driver amplifier. By changing the excitation pulse amplitude we can discriminate between detection noise and resonant response peaks in the spectrum. The long cavity responses (with reverberation time of about 5 ms) are received by the 2-nd piezoelectric transducer. The 2-nd piezoelectric transducer is also coupled to the cavity using oil. Its signal is amplified by an EG&G Princeton Applied Research 5113 model pre-amplifier and recorded by a LeCroy Wave Surfer 424 model 200 MHz digitizing oscilloscope with time step of 0.1 μs.

The computer connected to the oscilloscope saves the recorded signals by means of Lab View Software (National Instruments Corp., Austin, TX, USA). A 65 536 point Fast Fourier transform of the reverberation response is calculated by Matlab routines (The Mathworks, Natick, MA, USA). Further calculations involve identification of resonances and give the statistical properties discussed further in Sections 3 and 4.

The spectral density of the excitation pulse is shown in Fig. 4 together with the spectral density of the excited cavity dynamics detected at the receiving piezoelectric transducer.

Both the radius of the well and the width of the aluminum prism removed at the corner of cavity Nr. 2, as well as the diameters of the transducers that are attached to the samples are very close to 5 mm. This is approximately half the

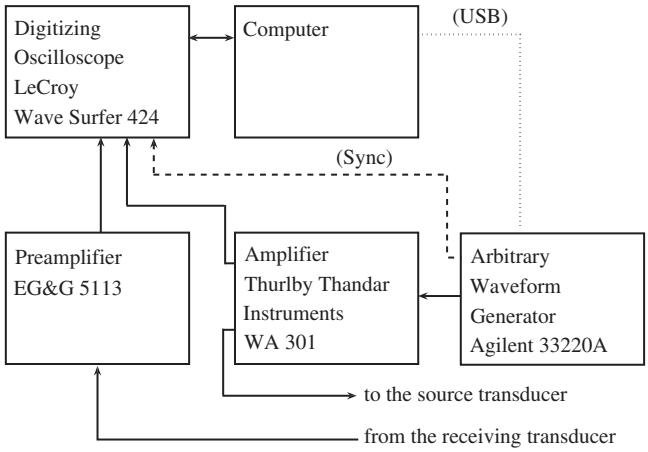

Fig. 3. Schematic of the experimental setup.

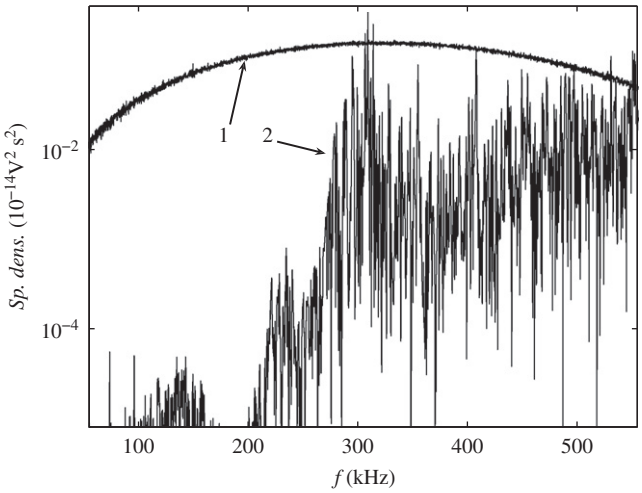

Fig. 4. Spectral densities of the short 2.5 μs pulse (one period of 400 kHz sine shape) used to excite the cavity oscillations (curve 1) and the 5 ms long response (curve 2) plotted over a broad frequency range. From the measurement on cavity Nr. 2.

wavelength of the transversal plane wave in aluminum at 200–450 kHz. The spectral density of the excitation pulse is peaked in this band (Fig. 4). The wavelength range of the 200. .450 kHz band used is approximately $1.6d$. $.0.7d$ for the fast (longitudinal) wave and $0.8d$. $.0.35d$ for the slow (transversal) wave. Here d is the size of aluminum cavities (see Fig. 1). Therefore, the main contribution to the detected density of resonances may come from "transverse-like" cavity oscillations. The "transverse-like" cavity modes should have a displacement component normal to the surface that can be detected by the compressional piezoelectric transducers. They are also the most likely to be excited by the source and received by the receiver which both have the diameter of approximately $0.25d$, which matches half the wavelength of the transverse wave inside the used frequency band. Resonances and corresponding wavefunctions of the complex metal 3D shape in general cannot be strictly divided into "transverse-like" and "longitudinal-like" ones e.g. due to transverse-longitudinal wave transformation at the complex cavity boundary. But transducers due to their size are more efficient in detecting displacement variations within the wavelength range corresponding to transverse waves at given frequencies. Even if so, that does not mean that "longitudinal-like" resonances are not detected.

In the band above 0.45 MHz (Fig. 4) more dense structure of resonances arises and unavoidably there is a situation reached when the resonance line width is of the order of the average spacing, so that individual cavity modes cannot be resolved any more.

3. Overview on RMT statistics in systems with time reversal invariance

The Gaussian Orthogonal Ensemble (GOE) is defined in RMT [2] as an ensemble of symmetric matrices that have identically distributed real random Gaussian elements and their statistical properties are invariant under orthogonal

matrix transformations. The distribution of nearest neighbor eigenvalue spacings for the members of the GOE describes the distribution of intervals between energy levels (resonant frequencies) of a class of semiclassical Hamiltonian physical systems [13]. However, RMT models such as GOE are applicable to the systems where an understanding in terms of semiclassics has not been achieved yet, such as complex nuclei or other many-body systems. So modelling a Hamiltonian with a random matrix has quite broad area of applications [3]. A symmetric matrix implies time reversal invariance in the system. The invariance of the statistical properties of the matrix ensemble under orthogonal transformations describes an ensemble of Hamiltonian matrices that cannot be decomposed into a matrix with separated diagonal blocks. Such a block decomposition [3] leads to additional "quantum numbers" and therefore to several independent sequences of energy levels. True non-regular (chaotic) resonances are described by only one "quantum number", related to the only quantity that is conserved—energy. This holds for Hamiltonian systems whose classical counterpart is fully chaotic [13]. Classical trajectories in the phase space of such systems are chaotically mixed so that energy is the only constant of motion.

The statistics of the wave resonances in chaotic cavities measured in the experiments described in Section 2 is expected to follow a GOE model. To characterize the statistics and to compare them with the model we will use the nearest neighbor eigenvalue (energy level, resonance) spacing distribution (NNSD) and the spectral rigidity (SR).

The NNSD gives the probability density of finding the value of the spacing between neighboring energy levels (cavity resonances) scaled by the average spacing in the sequence. The NNSD is normalized to unit area under the curve. If the energy levels (resonant frequencies) divide the given energy band into intervals randomly, as in case of regular (integrable) cavity waves, than the NNSD is a Poisson distribution (exponential distribution). Otherwise, if the observed resonances of chaotic cavity are described by the GOE model, the NNSD has a shape with a maximum, as shown by the dashed curve in Fig. 5. In this case NNSD is $\propto s\,\exp(-\pi s^2/(4s_{\mathrm{avg}}^2))$, where s is the nearest neighbor resonance spacing and s_{avg} is the average nearest neighbor resonance spacing. The average spacing s_{avg} is related to the Heisenberg time: $t_H = 1/s_{\mathrm{avg}}$.

The SR, Δ, is given [13] as follows:

$$\Delta = \left\langle \min_{A,B} \frac{1}{2L} \int_{-L}^{L} (N(E_C+\varepsilon) - A - B\varepsilon)^2 \,\mathrm{d}\varepsilon \right\rangle \tag{1}$$

or

$$\Delta = \left\langle \frac{1}{4L} \left[2\int_{-L}^{L} N^2(E_C+\varepsilon)\,\mathrm{d}\varepsilon - \frac{1}{L}\left(\int_{-L}^{L} N(E_C+\varepsilon)\,\mathrm{d}\varepsilon\right)^2 - \frac{3}{L^3}\left(\int_{-L}^{L} N(E_C+\varepsilon)\varepsilon\,\mathrm{d}\varepsilon\right)^2 \right] \right\rangle, \tag{2}$$

where A and B are free parameters chosen to minimize Δ in Eq. (1), $2L$ is the size of an energy band around the average energy value E_C. Brackets $\langle\ \rangle$ in Eqs. (1) and (2) imply averaging over a number of energy bands of size $2L$ centered at different values of E_C. The staircase function $N(E)$ is a step-like function that gives a number of energy levels below the value E. In case of aluminum cavities considered in this paper we will use function $N(f)$ giving amount of acoustic resonances below frequency f.

Deviation of this function around the best fitting line (Eq. (1)) is the "rigidity" of the spectra, measured by the SR. It is also important to notice that equivalent form of the SR (Eq. (2)) shows its similarity to standard deviation of $N(E)$ per

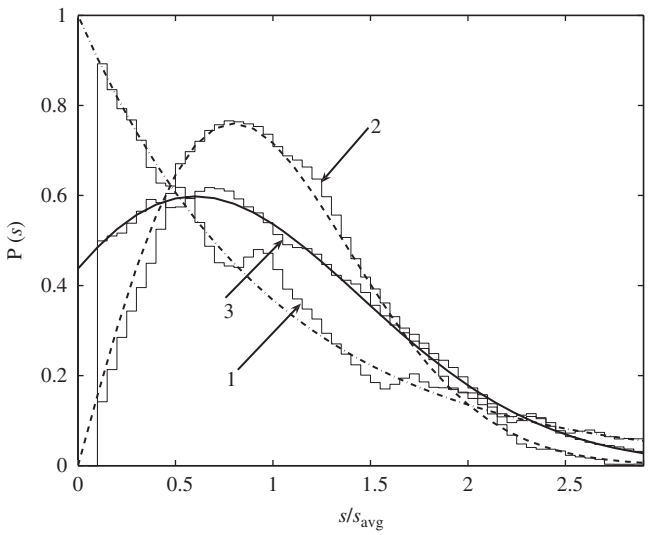

Fig. 5. The NNSD for GOE (dashed curve) and Poisson distribution (dash-dotted curve). Solution for NNSD according to [16] for the case of coexistence of GOE and random sequences of energy levels with a 3:1 density ratio, uniformly distributed within the same energy band (solid curve). Corresponding statistical simulations for random and GOE energy level sequences are shown as step-like functions 1 and 2, respectively. The NNSD obtained for coexistence of these two sequences is given by the step-like function 3.

interval $2L$. The important property of the SR is: if energy levels (resonant frequencies) divide the given energy band into intervals randomly, then the SR is proportional to the total size of the included small energy band $2L$, increasing exactly as $2L/(15s_{avg})$. While for energy levels distributed as a sequence of eigenvalues of the GOE the SR should saturate logarithmically with increasing L according to the prediction [13,14] for GOE. Unlike the NNSD, the SR accounts not only for amounts of spacings larger or smaller than average one, but also for the order in which large and small spacings appear on the scale larger than several s_{avg}.

The distributions originating from coexistence of independent energy level sequences can be derived analytically [15,16] by combining several independent energy level sequences in the observed energy band, or obtained via statistical simulation (see Fig. 5).

The important class of distribution models—distribution for incomplete sequences of energy levels may be also efficiently obtained via statistical simulation (Fig. 6). We simulated the GOE distribution accounting for levels lost in the detection by averaging the NNSD over a set of level sequences with GOE distributed nearest neighbor spacing. Each sequence consisted of 100 energy levels and a given fraction of levels (lost levels) was randomly removed before calculation of the NNSD.

From Fig. 5 we see that a pure sequence of eigenvalues of the GOE ensemble has a distribution that approaches the Poisson distribution after random levels are added (step-like function 3 and solid curve in Fig. 5). Similar transformation of the NNSD happens when a fraction of the sequence is lost in the detection (Fig. 6), although the intercept of the NNSD (amount of arbitrary small spacings) does not increase in this case. These trends are also seen in the spectral rigidity—the spectrum becomes more random (either due to adding randomly chosen levels or randomly removing the existing ones) and therefore more rigid (greater rigidity) in case of incomplete or mixed sequence of energy levels.

The GOE behavior in ultrasonic wave propagation has been found in volume (3D) rectangular aluminum blocks with slits, breaking the symmetry of the cavity [17]. The case of volume acoustic chaotic resonators with one symmetry plane has been studied as well. Weaver et al. [17,18] found that the NNSD in this case is consistent with distribution for 2 independent GOE distributed sequences of resonances (assumed related to odd and even wavefunctions) coexisting in the frequency band. This implies that the total sequence of the resonant frequencies can be labelled with new "quantum number" either n_p=0 or 1 related to the conservation of parity in addition to the mentioned "quantum number", related to conservation of energy.

The difference in spectral fluctuations for cubic aluminum cavity and the same cavity with removed small octant at the edge has been detected [19]. In similar way the gradual transition from the resonator that has a mirror-like symmetry to fully chaotic resonator has been studied and the corresponding evolution of the NNSD (approaching the GOE model) was observed experimentally in anisotropic quartz blocks [20]. More complex GOE based systems (2D resonators), made out of plates were studied in [5,6]. In particular the NNSD in [5,6] is actually caused by coexistence of independent GOE sequences of approximately equal densities in the same frequency band. Identification of the modes that belong to each subsequence (e.g. odd and even) was done by studying the sensitivities of resonance line widths to external parameters such as temperature and pressure [5].

This leads to the important conclusion that the symmetries (additional classical constants of motion or additional "quantum numbers") of the Hamiltonian can be experimentally identified by observing the NNSD and the SR. The extra

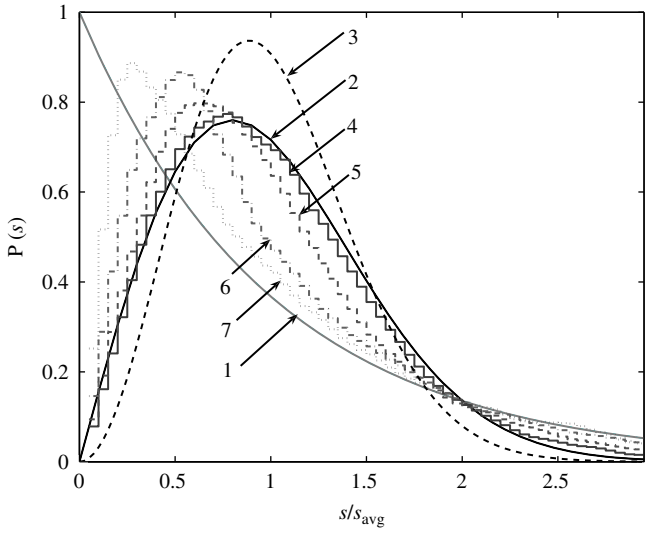

Fig. 6. NNSD for random arrangement of energy levels (exponential distribution, curve 1), GOE (curve 2) and GUE (curve 3). Statistical simulations shown here as step-like functions 4, 5, 6 and 7 correspond, respectively, to 10, 25, 50 and 75 percent of energy levels lost in generated sequence with NNSD due to GOE model. GOE distributions with lost levels shown in this figure are very similar to those given in work [8] by Enders et al.

symmetries cause independent eigenspectra to overlap and the energy levels are allowed to fall closer to each other. The associated NNSD will tend to follow the Poisson distribution. Removing symmetries leads in general to deviation of the NNSD from Poisson distribution and approaching the GOE model, where energy levels do not tend to fall close to each other (Fig. 5), and the SR saturates logarithmically.

But the mentioned symmetries that lead to new "quantum numbers" are not the only symmetries involved. In principle also the time reversal invariance can be broken. Than the system can still be described by the Hamiltonian approach now based on a Hermitian matrix. This applies to e.g. the cases where regular "rotating" disturbance enters the wave equation [21,22] and the system evolves in a closed cycle making the dynamics irreversible in time. The distribution of energy levels for this case is described by eigenvalue statistics for the matrix ensemble with statistical measures that are invariant under unitary transformations (GUE) [13,14]. The GUE model, where $p(s) \propto s^2 \exp(-4s^2/(\pi s_{\text{avg}}^2))$, curve 3 in Fig. 6 gives even greater repelling of energy levels. The eigenspectrum becomes less rigid, meaning also that the logarithmic saturation of the SR occurs at a lower level. So breaking of the time reversal invariance leads to even greater repelling of energy levels than in all earlier mentioned cases (GOE sequence of energy levels and several coexisting independent GOE sequences).

By carefully measuring the NNSD and the SR it is possible to identify the symmetry properties of the system. A promising application is for example the analysis of the spectra of complex molecules in order to identify their symmetry [23]. Also many complex classical mechanical systems could be monitored based on GOE or GUE statistics of ultrasonic resonances.

The fact that not all resonances have been detected ("lost modes") should be accounted for in a realistic experiment. Accounting for a fraction of resonances that are not detected plays an important role in analysis of our experiment. We will see that it is still possible to identify the essential features of the underlying statistical distributions in the experiment using simulated distributions (as in Fig. 6) for incomplete sequences of resonances. Comparison of the NNSD obtained in experiment to those in Fig. 6 allows quantitative estimation of the amount of lost resonances.

The possibility to study the relation between level statistics and time reversal invariance in a single system motivated us to perform time reversal experiment [10] in the aluminum samples. The experiments show directly how efficiently the wave dynamics in the model chaotic cavity (that conforms GOE statistics) can be reversed depending on how long the excitation pulse was dispersed while pulse energy was travelling chaotic trajectories in the cavity. We can compare then the time scale of the Heisenberg time t_H related to the level spacings to the behavior of our time reversal experiment.

4. Discussion and analysis of the results

4.1. Division of energy between cavity waves: distributions of intensity transmission coefficients and resonance line widths

If a finite amount of energy in each excitation pulse in the chosen frequency band is shared randomly between the cavity waves, then the distribution of the intensity transmission coefficient in the appropriately small frequency band is expected to be exponential. The normalized intensity distribution (NID) obtained for cavity Nr. 1 is shown in Fig. 7. The results agree with an exponential dependence if the distribution is evaluated in a small enough frequency band (60 kHz wide, contains about 30 resonances). For broader frequency bands the distribution is a mixture of exponentially distributed intensities with different average values, resulting in an overall non-exponential intensity distribution.

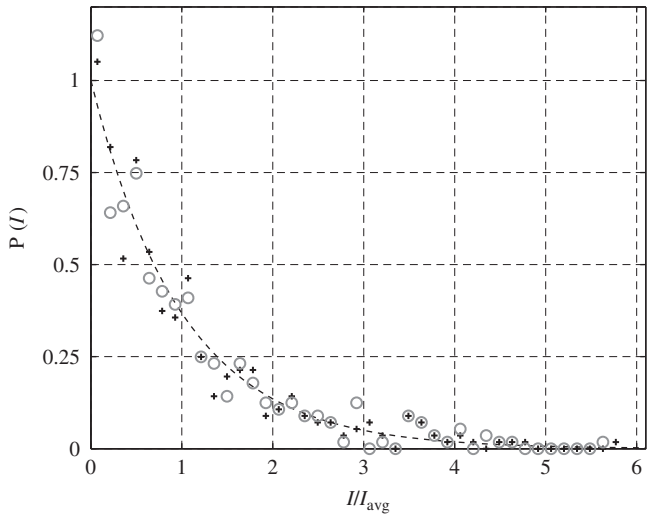

Fig. 7. Typical normalized intensity distribution for 60 kHz wide frequency band. The cross and round symbols give distributions for different signal amplitudes. From the spectral density of the recorded responses of cavity Nr. 1 in 0.27..0.33 MHz band. I_{avg} is the average intensity in the band. Dashed curve shows exponential distribution.

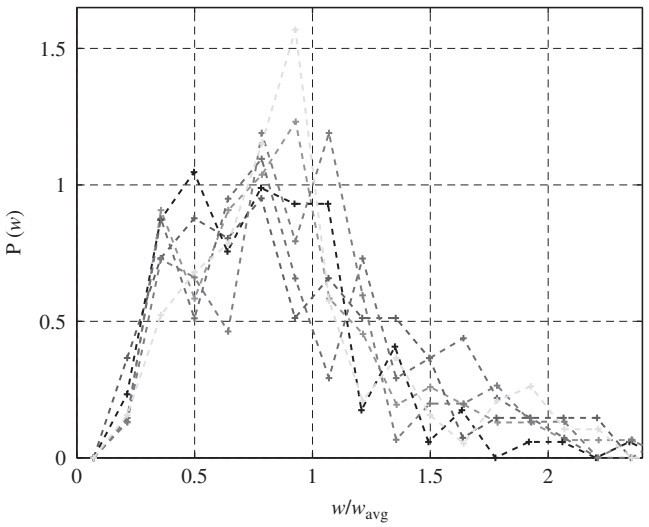

Fig. 8. Resonance line width distributions for measurements at different positions of source and receiver for cavity Nr. 2. w_{avg} is the average resonance line width.

As mentioned above, the distribution of the intensity transmission coefficients and resonance widths are related to each other and overall related to the distribution of pulse intensity between different kinds of cavity waves. In case the detected resonances form a single GOE sequence of resonances or are a major part of it the resonance width distribution is expected to be peaked around a single average value. This is more or less in agreement with the distributions obtained for cavity Nr. 2 at different locations of source and receiver. They are shown in Fig. 8. The value of the average resonance width w_{avg} is about 300–400 Hz. So the ratio of the average resonance width to the average nearest neighbor resonance spacing determined from experimental data is approximately 0.2.

4.2. Statistical properties of sequences of resonances due to RMT: NNSD and SR

The statistics mentioned in the previous section describes how finite pulse intensity is shared. Now we proceed to calculating the RMT statistics from the measured cavity responses. As mentioned in the introduction, it involves studying how the values of resonant frequencies are distributed themselves or more precise how do they divide fixed finite frequency band into intervals. We take a broad frequency band of 200. .250 kHz with an almost constant resonance density and calculate the NNSD. The result calculated from the experimental time traces for cavity Nr. 2 is shown in Fig. 9. We see that the results do not agree with the pure model of the GOE, but do agree much better with the distribution where a loss of 25 percent of the resonances is accounted for. The error bars in Fig. 9 are based on calculations from measurements performed for different positions of receiver and source on the surface of the sample. From the NNSD we obtain an average nearest neighbor spacing for both cavities of about 1.8 kHz. This gives an estimate for Heisenberg time: $t_H \approx 556\,\mu s$. However, there can be more resonances missing, or independent sequences of resonances present in the case of cavity Nr. 1. Lost resonances can lead to a smaller value of the average nearest neighbor spacing and a larger apparent Heisenberg time.

Fig. 10 shows the experimentally determined staircase function for different alignment of the transducers. The best alignment enables to observe the largest amount of resonances and is used in determining the spectral rigidity. To compensate for slow increase of density of resonances with frequency an unfolding procedure [24] has been applied to the staircase functions using a fit of the staircase functions with a smooth cubic polynomial (Fig. 10).

From the Fig. 11 we see that SR satisfactory agrees with a GOE model [13] for averaging over the frequency bands of 2..10 average spacings in case of cavity Nr. 2. It is, however, slightly larger than predicted by the model probably due to a fraction of lost resonances. The spectral rigidity calculated from the data of the same experiment for cavity Nr. 1 is systematically larger. The error bars in Fig. 11, the same as in Fig. 9, are based on calculations from cavity responses recorded at different positions of receiver and source on the surface of the sample. SR values for both cavities agree better with the GOE model (that involves logarithmic saturation of SR) than with the case of random division of the frequency band into intervals by cavity resonances (straight dashed line in Fig. 11). Solid curve that shows the case of GOE model with 25 percent of eigenvalues lost is also shown in Fig. 11. It offers reasonably good fit to the spectral rigidities determined from the experiment. This solid curve in Fig. 11 has been calculated as SR for sequence of eigenvalues of large (5000×5000) real symmetric matrix when 25 percent of eigenvalues have been randomly removed from the sequence.

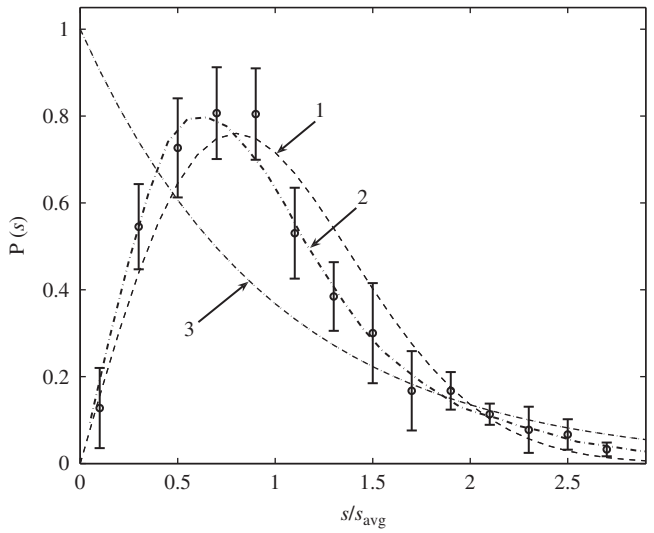

Fig. 9. The nearest neighbor resonance spacing distribution (NNSD) for cavity Nr. 2. Experiment is shown as points with error bars. Curve 1 shows the distribution expected due to GOE model. Curve 2 accounts for 25 percent of eigenvalues lost in GOE model distribution. The Poisson distribution is shown by curve 3.

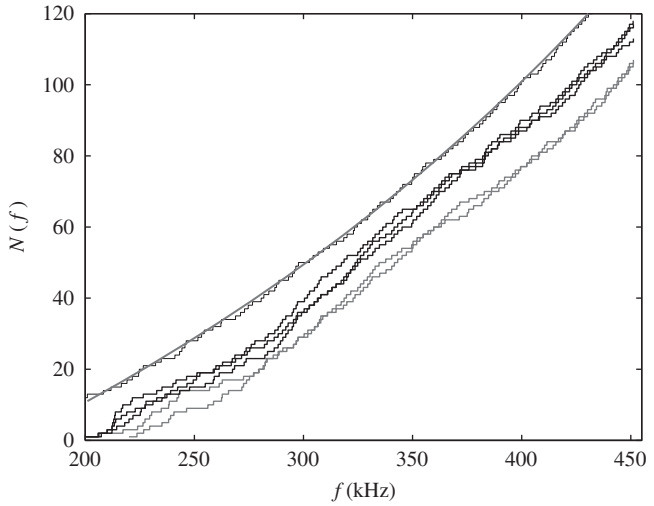

Fig. 10. The experimentally determined staircase functions $N(f)$ for cavity Nr. 2 for different coupling of the transducers with the cavity at certain fixed positions of source and receiver. The staircase function and smooth cubic polynomial fitting it (top curves).

4.3. Efficiency of excitation pulse reconstruction in time reversal experiments

There is a natural decay of acoustic energy density in the cavities due to absorption in the aluminum, the loss to the piezoelectric transducers, and some coupling to the support and surrounding air that causes departure from time reversal invariance. We will see that in the experiments the oscillations can be observed for a time considerably longer than the Heisenberg time, as well as time-reversal experiment can be performed on time scales beyond the Heisenberg time, so the NID, NNSD and SR still provide a basis for the characterization [2].

Time reversal experiment, as e.g. described in [10] in general and worked out for a closed chaotic system in [11] could be a clear measure of time reversal invariance for acoustic waves in a chaotic cavity. As outlined in [11], a single transmitter-receiver pair is sufficient to perform a time-reversal experiment in a closed cavity. We performed such time reversal experiments using the same set up and samples used in the statistical analysis described in previous sections. In this experiment each part of the cavity response shown in Fig. 12 was recorded separately. Then each track has been scaled to appropriate integer numbers, which were downloaded into the memory of the AWG. So the AWG could replay the recorded oscillation track in the reversed time direction (oscillations that arrived first are being released last). Each of the responses to the 300 μs long reversed tracks (Fig. 12) gives a clear reconstruction of the original short pulse (Fig. 13).

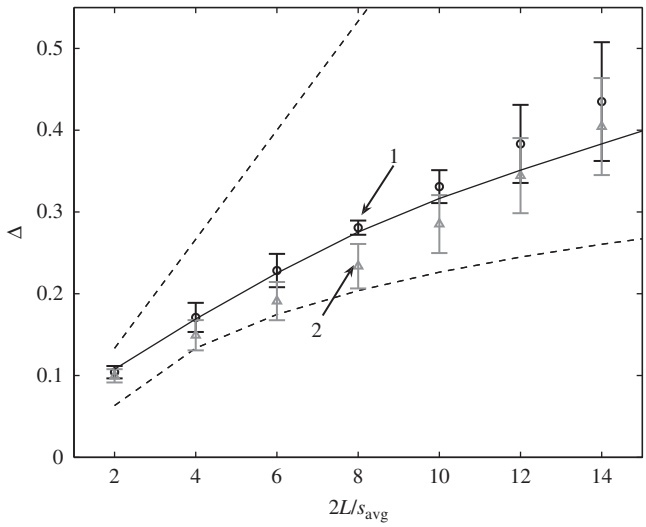

Fig. 11. The spectral rigidity for cavity Nr. 1 (circles with error bars, marked as "1") and cavity Nr. 2 (triangles with error bars, marked as "2"). The GOE model that involves logarithmic saturation of SR and the case of random division of the frequency band into intervals are shown as dashed curve and dashed line, respectively. Solid curve shows the case of GOE with 25 percent of eigenvalues lost.

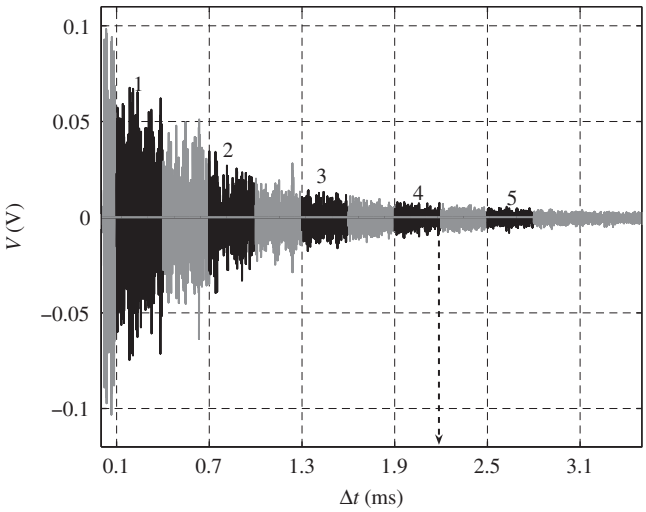

Fig. 12. Cavity response upon the exciting pulse at $\Delta t = 0$, for cavity Nr. 2.

The arrows in Figs. 12 and 13 demonstrate that after the generation of the particular reversed oscillation track (track 4) one has to wait until the refocused image of the excitation pulse exactly the time delay Δt between the original excitation pulse and the end of the recorded oscillation track. Thus we explicitly see time reversed wave propagation in our aluminum cavities. Five of 300 μs long oscillation tracks in Fig. 12 that are to be replayed backwards in time are marked with numbers (from 1 to 5). The corresponding reconstructions of the excitation pulse (which appear as a response to certain reversed oscillation track) in Fig. 13 are marked with the same numbers. We observe the reconstruction peak on the background of noisy decaying signal (Fig. 13) due to the fact that only short finite part of the response is being time reversed.

Fig. 14 shows the amplitude of the reconstructed pulse, normalized to σ_i, the mean square average of the signal amplitude in the reversed 300 μs long oscillation track used for excitation. σ_i is proportional to the square root of the energy contained in 300 μs signal section driving the exciting transducer. $\sigma_{\max}$ in Fig. 14 is the maximum of all $13\sigma_i$ related to 13 points in Fig. 14. The normalized amplitude characterizes the efficiency of energy focusing in the time reversal experiment with a given time delay of the end of the recorded oscillation track with respect to the excitation pulse. We can expect from Fig. 14 that the amplitude of the reconstructed pulse decays exponentially with delay time. This can be explained simply as absorption of acoustic energy during the time it is stored in the cavity, before the energy is refocused into a reconstructed pulse. However, for the normalized amplitude of the reconstructed pulse shown in Fig. 14 this behavior does not extend down to smaller delay times (at least does not extend with the same decay constant). The small

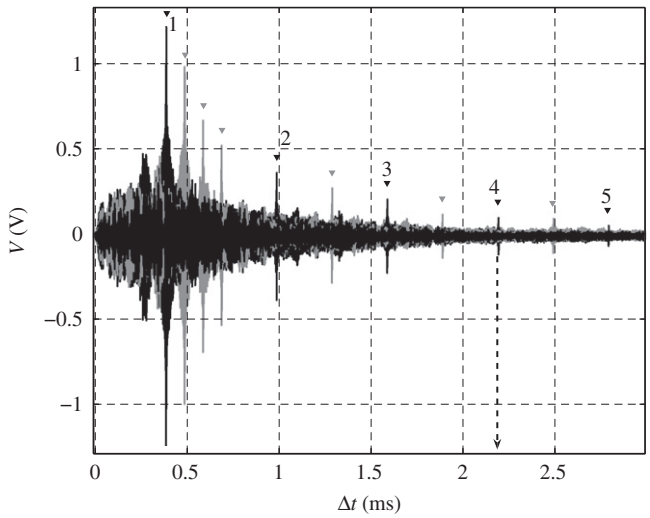

Fig. 13. The reconstruction of the dispersed input pulse by time reversal of the recorded signal for cavity Nr. 2. The experiment shows to be working for time delays much longer than the Heisenberg time.

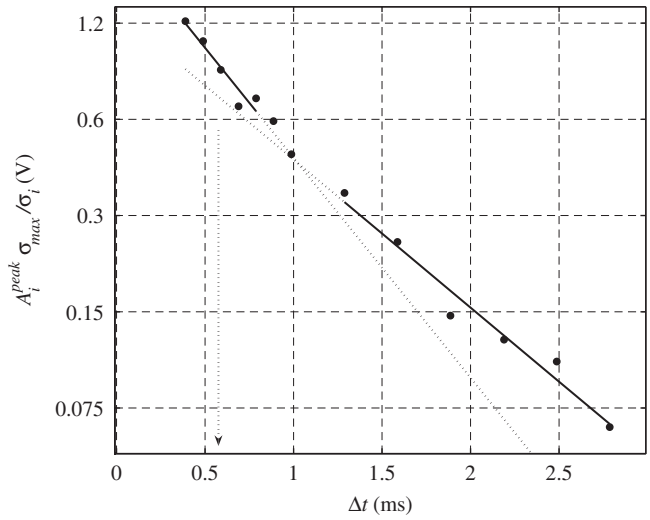

Fig. 14. Normalized amplitude of the refocused excitation pulse depending on the time delay of the reversed oscillation trace. Closed circles show result of the experiment on cavity Nr. 2. The solid lines show linear least square fits using the first five and the last five points.

delay times correspond to shorter and therefore probably less chaotic trajectories. The estimate of the Heisenberg time is marked with an arrow in Fig. 14.

We made the reversed track as short as possible (300 μs), just enough to insure good detection of the maximum in reconstruction peak. This enables to judge the efficiency (per input energy) of the refocused pulse as function of the time delay.

Change in the slope shown in Fig. 14 still remains to certain degree a challenge to understand. It can be related to the fact that longer scattering times correspond to better approach to equilibrium energy distribution between cavity modes what affects the reversibility of the wave dynamics.

5. Conclusions

Distributions of intensity transmission coefficients studied in the narrow frequency bands confirm random division of pulse intensity between the cavity waves for both studied cavities. Division of the frequency band into intervals by cavity resonances for cavity Nr. 2, characterized by the NNSD, is found in agreement with prediction of RMT for GOE when accounting for a fraction of lost resonances (about 25 percent). The SR shows behavior close to the GOE model that involves logarithmic saturation of the SR. Curve that shows SR in case of GOE model with 25 percent of eigenvalues lost offers even

better fit to the spectral rigidities determined from the experiment. The SR, calculated from the data of the experiment for a symmetric cavity is systematically larger than in the comparable case of an asymmetric cavity. This agrees with the concept of coexistence of odd and even independent sequences of resonances. The normalized amplitude of the reconstructed pulse in the time reversal experiment deviates from exponential dependence on the time delay if the last one is getting smaller and approaches the Heisenberg time (inverse of the nearest neighbor spacing).

It is necessary, however, to explain why the amount of lost resonances found in present work is noticeably higher than in earlier reports like [9]. Work [9] reports extremely optimized experiment:

a. Authors use aluminum plate resonators instead of volume ones in our work.
b. Authors use vacuum chamber enclosing the sample to increase isolation and therefore quality factor of the resonances.
c. Probably better support mechanism is used as well.

We report experiments that have been done at normal room conditions in air with support of the sample not entirely optimized. Therefore, a bit worse resonance detection conditions are indeed in place. However, it makes sense to explore possibility of calculations of RMT statistics from experiments on arbitrary samples at non-optimized conditions, especially when searching for probable future applications in mechanical engineering.

Acknowledgment

This work is part of the research program of the "Stichting voor Fundamenteel Onderzoek der Materie (FOM)", which is financially supported by the "Nederlandse Organisatie voor Wetenschappelijk Onderzoek (NWO)".

References

[1] D.E. Newland, *An Introduction to: Random Vibrations, Spectra & Wavelet Analysis*, third ed., Longman Scientific & Technical, New York, 1993.
[2] H.-J. Stöckmann, *Quantum Chaos*, Cambridge University Press, Cambridge, 1999.
[3] T. Guhr, A. Müller-Groeling, H.A. Weidenmüller, Random-matrix theories in quantum physics: common concepts, *Physics Reports* 299 (1998) 189–425.
[4] M.R. Schröder, Eigenfrequenzstatistk und Anragungsstatistik in Raümen, *Acustica* 4 (1954) 456–468.
[5] K. Schaadt, Experiments on Acoustic Chaology and Statistical Elastodynamics, PhD Thesis, University of Copenhagen, 2001.
[6] A. Andersen, C. Ellegaard, A.D. Jackson, K. Schaadt, Random matrix theory and acoustic resonances in plates with an approximate symmetry, *Physical Review E* 63 (2001) 066204.
[7] K.K. Lehmann, S.L. Coy, The Gaussian orthogonal ensemble with missing and spurious levels: a model for experimental level-spacing distributions, *The Journal of Chemical Physics* 87 (1987) 5415–5418.
[8] J. Enders, T. Guhr, N. Huxel, P. von Neumann-Cosel, C. Rangacharyulu, A. Richter, Level spacing distribution of scissors mode states in heavy deformed nuclei, *Physics Letters B* 486 (2000) 273–278.
[9] T.N. Nogueira, J.C. Sartorelli, M.P. Pato, C. Ellegaard, Missing levels in acoustic resonators, *Physical Review E* 78 (2008) 055201-1–055201-4.
[10] M. Fink, Time reversed acoustics, *Physics Today* 50 (1997) 34–40.
[11] C. Draeger, M. Fink, One-channel time reversal of elastic waves in a chaotic 2D-silicon cavity, *Physical Review Letters* 79 (1997) 407–410;
C. Draeger, M. Fink, One-channel time-reversal in chaotic cavities: theoretical limits, *The Journal of the Acoustical Society of America* 105 (1999) 611–617.
[12] H.H. Demarest, Cube-resonance method to determine the elastic constants of solids, *The Journal of the Acoustical Society of America* 49 (1971) 768–775.
[13] M.V. Berry, The Bakerian lecture, 1987: quantum chaology, *Proceedings of the Royal Society of London, Series A: Mathematical and Physical Sciences* 413 (1987) 183–198.
[14] M.V. Berry, Semiclassical theory of spectral rigidity, *Proceedings of the Royal Society of London, Series A: Mathematical and Physical Sciences* 400 (1985) 229–251.
[15] N. Rosenzweig, C.E. Porter, "Repulsion of energy levels" in complex atomic spectra, *Physical Review* 120 (1960) 1698–1714.
[16] M.V. Berry, M. Robnik, Semiclassical level spacings when regular and chaotic orbits coexist, *Journal of Physics A: Mathematical and General* 17 (1984) 2413–2421.
[17] R.L. Weaver, Spectral statistics in elastodynamics, *The Journal of the Acoustical Society of America* 85 (1989) 1005–1013.
[18] D. Delande, D. Sornette, R. Weaver, A reanalysis of experimental high-frequency spectra using periodic orbit theory, *The Journal of the Acoustical Society of America* 96 (1994) 1873–1880.
[19] C. Ellegaard, T. Guhr, K. Lindemann, H.Q. Lorensen, J. Nygård, M. Oxborrow, Spectral statistics of acoustic resonances in aluminum blocks, *Physical Review Letters* 75 (1995) 1546–1549.
[20] C. Ellegaard, T. Guhr, K. Lindemann, J. Nygård, M. Oxborrow, Symmetry breaking and spectral statistics of acoustic resonances in quartz blocks, *Physical Review Letters* 77 (1996) 4918–4921.
[21] M.V. Berry, M. Robnik, Statistics of energy levels without time-reversal symmetry: Aharonov–Bohm chaotic billiards, *Journal of Physics A: Mathematical and General* 19 (1986) 649–668.
[22] M.V. Berry, R.G. Chambers, M.D. Large, C. Upstill, J.C. Walmsley, Wavefront dislocations in the Aharonov–Bohm effect and its water wave analogue, *European Journal of Physics* 1 (1980) 154–162.
[23] G. Grossia, L. Peroncelli, N. Rahman, Statistics of energy levels in the quantum treatment of an elementary reaction, *Chemical Physics Letters* 313 (1999) 639–646.
[24] F. Haake, *Quantum Signatures of Chaos*, second ed., Springer Series in Synergetics, 2001, pp. 58–60.